**ORIGINAL ARTICLE** 



# Computational exploration of nigerian bioactive compounds as potential inhibitors of septic shock

Yemisi Elizabeth Asibor<sup>1\*</sup>, Dayo Felix Latona<sup>1</sup>, Banjo Semire<sup>2</sup>

#### Edited by

Angela Johana Espejo Mojica editorus@javeriana.edu.co

1. Osun State University, Department of Pure & Applied Chemistry, Osogbo, Nigeria. 2. Computational Chemistry Laboratory, Department of Pure and Applied Chemistry, Ladoke Akintola University of Technology, Ogbomoso, Nigeria.

\*yemisi.asibor@uniosun.edu.ng

Received: 28-11-2025 Accepted: 19-09-2025 Published online: 13-11-2025

Citation: Asibor YE, Felix-Latona D, Semire B. Computational exploration of nigerian bioactive compounds as potential inhibitors of septic shock, *Universitas* Scientiarum, 30: 224-246, 2025 doi: 10.11144/Javeriana.SC30.ceon

Funding: n.a

**Electronic supplementary** material: n.a.



#### **Abstract**

Septic shock is a fatal medical condition characterized by severe hypotension or elevated lactate levels as a consequence of sepsis. Septic shock occurs as a result of pathogenic bacterial and viral infections. In this study, twenty-eight ligands from natural plant sources were computationally screened for their ability to suppress septic shock via interaction with the protein Catechol-O-Methyltransferase (COMT) (PBD: 4XUC), as revealed by Molecular Docking, PASS, ADMET, and DFT analyses. The molecular docking results showed that the assessed ligands Capsaicine (L5) and Gingerenone A (L6) had binding affinities of -7.9 kcal/mol and -8.1 kcal/mol with an inhibition constant of 1.60 μM and 1.14 μM respectively, while the standard drugs dobutamine and dopamine had had binding affinities of -7.0 kcal/mol and -5.8 kcal/mol and inhibition constants of 7.35 µM and 55.77 µM. PASS analysis revealed that L5 and L6 had higher active probability values of 0.357 and 0.346, and the ADMET analysis ranked L5 and L6 as the best ligands. Finally, the DFT assessment showed that L5 and L6 had a band gap of 5.58 and 4.20. All the analyses showed that the two compounds, L5 and L6, had an improved binding affinity with the receptor over that of the two assessed approved drugs, dobutamine and dopamine.

**Keywords:** ADMET; Bioactive compounds; DFT; Molecular docking; PASS.

### 1. Introduction

Daily, infectious diseases claim thousands of lives worldwide [1]. Staphylococcus aureus is a prominent cause of infections leading to toxic shock syndrome, toxic sepsis, abscess, food poisoning, third-grade burns, traumatic ulceration, surgical incision, bed sores, and trophic ulcers [2, 3]. The Greek term for decomposition or rotting is where the word sepsis originates. Its usage dates back more than 2 700 years, when it first surfaced in poetry by Homer. Hippocrates and Galen also utilized it [4]. Sepsis is the body's systemic reaction to a severe infection, resulting in a complex web of pathogen-host interactions and an increase in inflammatory mediators [5].

Sepsis is characterized by the presence of infection and a systemic inflammatory response to infection. Numerous inflammatory pathways are activated, raising the odds of dying from it. For instance, septic shock is a condition involving hypoxia and tissue distress due to the presence of pathogenic germs in the blood [6]. Malignant tumors, organ transplantation, AIDS, radiation therapy, burns, sores, polytrauma, diabetes mellitus, hepatic failure, renal failure, malnutrition, catheters or other invasive devices, urinary catheters, and other conditions can all cause sepsis [7–9]. Since sepsis progresses into septic shock, it is associated with a significant increase in mortality. Sepsis combined with hypotension is suggestive of septic shock. Early detection and



treatment are essential [10, 11]. Numerous contemporary methods, including albumin, sublingual microcirculatory, fluid resuscitation, norepinephrine, dobutamine, and calcium sensitisers (such as levosimendan) are used in septic shock resuscitation [12].

Medicinal plant use to treat septic shock arises as an alternative to counter the detrimental side effects of current treatments on patients. The treatment of numerous diseases with phytochemicals has developed notably over the past few decades [13]. Because plants are broadly available and have fewer side effects, herbal remedies are currently gaining application [14]. Iranian native herbs include figworts, *Lawsonia inermis*, *Eucalyptus sp.*, *Punica granatum* L. (pomegranate), coriander, and *Descurainia sophia*, which are sources of medically valuable bioactive compounds. Also, derived from Traditional Chinese Medicine (TCM), Shenfu decoction and, later, Shenfu injection (SFI) are made from *Aconitum carmichaelii* Debx. (known as fuzi) and *Talinum paniculatum* Jacq. (known as hongshen). With good curative outcomes, SFI serves to treat several disorders, such as heart failure, shock, and sepsis [15, 16].

A 2020 World Health Organization (WHO) report states that sepsis affects over 50 million people globally and accounts for over 10 million fatalities (WHO 2020). The Korea Centers for Disease Control and Prevention (KCDC) reported that in 2022, there were 5235 sepsis-related deaths in South Korea and 25 697 patients who underwent sepsis-related testing [17]. The European Society of Anaesthesiology and Intensive Care (ESAIC) estimates that sepsis causes around 50 million cases and 11 million fatalities globally annually, signifying one-fifth of all deaths worldwide. Nearly 700 000 people die from sepsis each year in Europe, of which 3.4 million instances are avoidable [18].

In silico tools facilitate the investigation and elucidation of chemical-protein and protein-protein interaction mechanisms [19–21]. We used molecular docking to simulate the interaction of drug-effective molecules with disease targets, exploring disease molecular mechanisms, pharmacokinetics [21], drug resistance [22], and other action mechanisms. The key active components in SFI for the treatment of sepsis were ginsenoside Rf, ginsenoside Re, and karacoline, as demonstrated by a molecular docking study [23]. The identification of core targets for prospective treatments with SFI included LGALS3, BCHE, AKT1, and IL2. [23]. The primary goal of this work was to computationally screen bioactive chemicals from Nigeria for possible inhibitors of septic shock and sepsis.

#### 2. Materials and methods

With a 64-bit operating system and an x64-based processor, the system used for the docking research and other online drug design tools ran on a 1.00 GHz and 1.19 GHz processing setup. With 8.00 GB of RAM installed, the machine could accommodate 7.77 GB of usable memory. The canonical SMILES of twenty-eight (28) compounds and standard medications were downloaded and saved from the PubChem database.

The inhibitory actions of twenty-eight (28) phytochemicals against septic shock (PDB ID: 4XUC) were investigated in this study. Two standard medications (Dopamine and Dobutamine) were also included as comparators. The 28 assessed ligands were considered due to their documented inhibitory actions against septic shock and outcomes from randomized trials. Molecular docking analyses were performed with the 28 ligands, plus the two standard drugs, and the protein Catechol-O-Methyltransferase (PDB ID: 4XUC). Then, the web server https://pharmaexpert.ru/passonline/ was queried to predict the activity spectra of substances (PASS) for the ligands with good binding affinity. Additionally, the ligands' ADMET (Absorption, Distribution, Metabolism,

Excretion, and Toxicity) assessments were conducted using SwissADMET (http://lmmd.ecust.edu.cn/admetsar2/result/?tid=684417). The molecular descriptors characterizing the actions of the investigated compounds were assessed using the optimal structures of the phytochemicals, as determined by DFT simulations. Becke's three-parameter hybrid functional with Lee, Yang, and Parr's correlation (B3LYP) was employed in DFT [24, 25]. The optimization unfolded using the 6-31+G(d,p) basis set and the Spartan 14 quantum chemistry program [26].

#### 2.1. Ligand structural data

The 3D structural data files (SDF) of twenty-eight (28) tested bioactive ligands from various natural plant databases and the control compounds, Dopamine and Dobutamine, were obtained from the PubChem Database (https://pubchem.ncbi.nlm.nih.gov). All there compounds were tested for their ability to suppress septic shock in trough interaction with the protein Catechol-O-Methyltransferase (COMT) (PBD: 4XUC) [27].

### 2.2. Target protein structural data

The protein data bank (RCSB) (http://www.rcsb.org/pdb) provided the synthesis and evaluation of heterocyclic catechol of catechol-O-methyltransferase (COMT) (PBD: 4XUC, 1.80Å), which was downloaded in PDB format (**Fig. 1**). To prevent unwanted molecular interactions and to ensure that no molecules obstructed the target proteins' possible binding sites during molecular docking, employing the Discovery Studio software version 2020, we removed all water molecules, heteroatoms, and undesirable complexes from the downloaded protein crystal structures. The Volume, Area, Dihedral Angle Reporter (VADAR) web server served to create Ramachandran plots that illustrate the characteristics of the receptors under investigation. The Ramachandran plot of the protein shows that it is usable (**Fig. 2**).

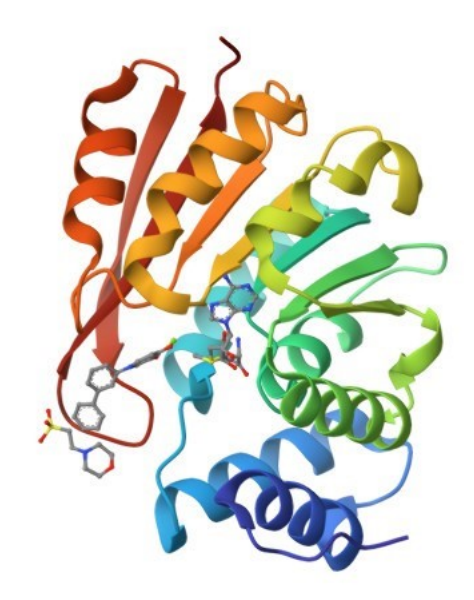


**Figure 1.** Crystal structure of the protein Catechol-O-Methyltransferase (COMT) (PDBID: 4XUC) (https://www.rcsb.org/structure/4XUC)

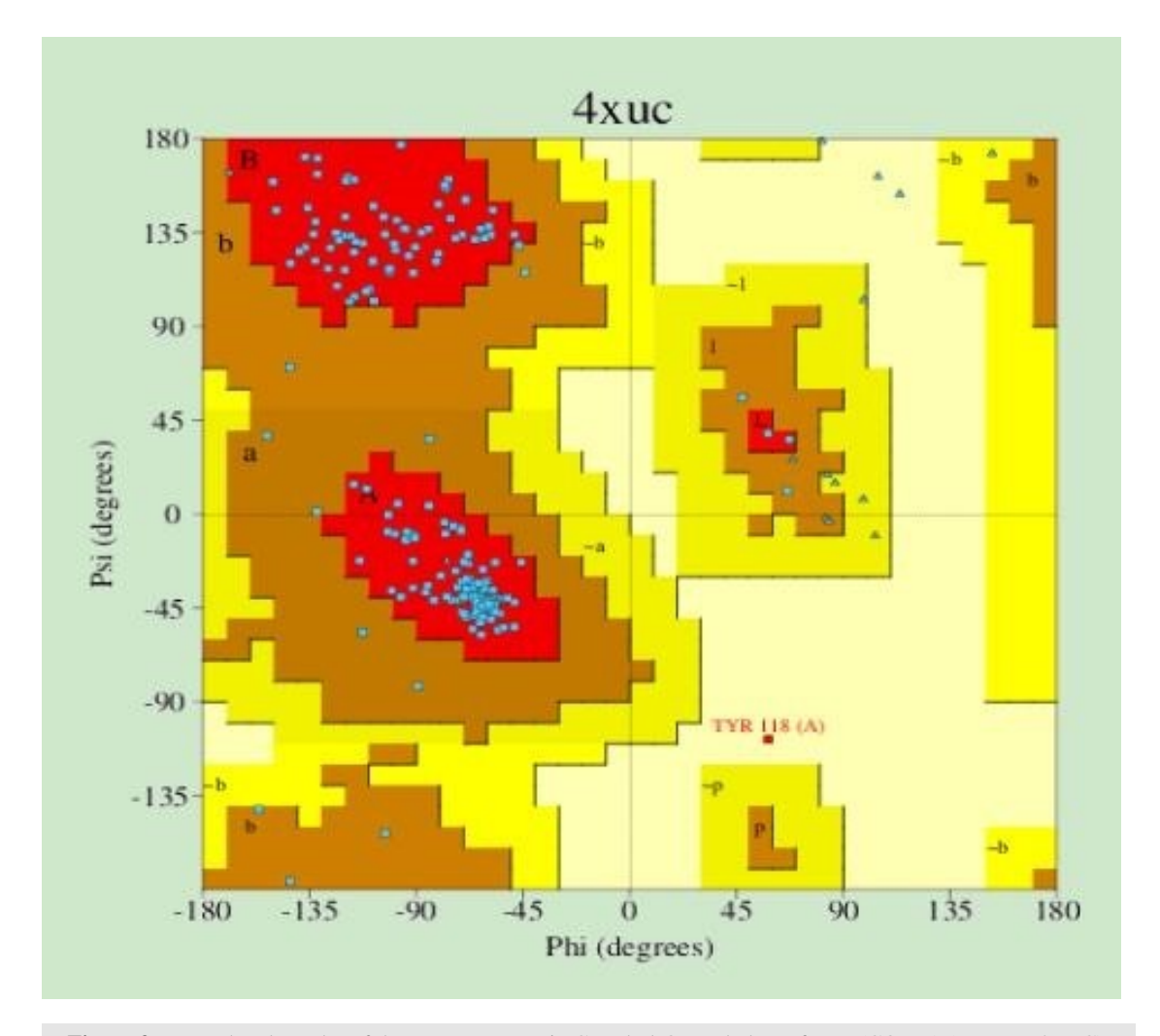
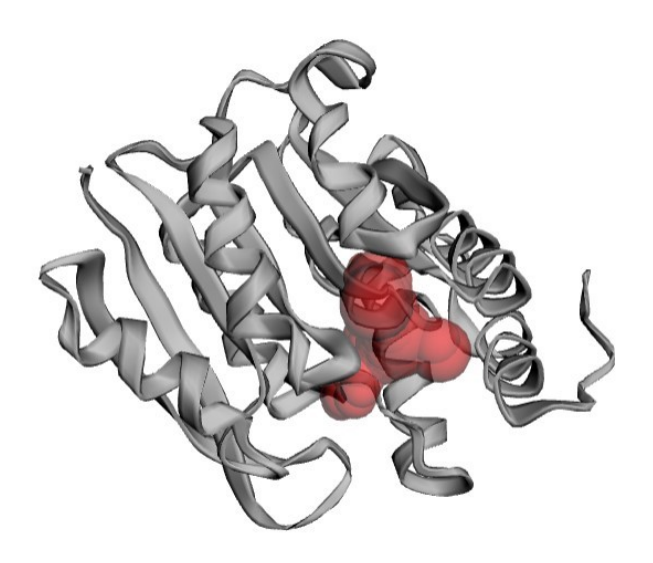


Figure 2. Ramachandran plot of the recepetor protein Catechol-O-Methyltransferase (COMT) (PDB ID:4UXC).

#### 2.3. Receptor's active site determination

The resolution of the crystal structure of the protein Catechol-O-Methyltransferase - COMT (PBD: 4XUC) [27] was 1.80Å, and the protein's binding pockets, ligand interactions, and active sites' amino acid residue compositions were determined with the tools Computed Atlas for Surface Topography of Proteins (CASTp) (http://sts.bioe.uic.edu/castp/index.html?2011) [28] and Biovia Discovery Studio (2019). Protein binding sites were defined using the obtained grid size during docking. This binding pocket, binding site analysis, ligand interactions, and all amino acid residues/interactions in the active sites of (PDB: 4XUC) (**Fig. 3**), were established using the Computed Atlas for Surface Topography of Proteins (CASTp) (http://sts.bioe.uic.edu/castp/index.html?2011) [28] and Biovia Discovery Studio (2019). The amino acids in COMT (PDB ID: 4XUC) active sites are Met A:91, Val A:92, Leu A:115, Gly A:116, Ile A:141, Asn A:142, Ser A:169, Cys A:145, Tyr A:118, Cys A:119, Tyr A:121, Ser A:139, Glu A:140, Gly A:167, Ala A:118 [29,30].



**Figure 3.** Binding pocket structure of Catechol-O-Methyltransferase (COMT) (PDB ID:4XUC). (CASTp 3.0, Computed Atlas of Surface Topography of proteins, sts.bioe.uic.edu/castp/index.html)

## 2.4. Molecular docking

Energy was minimized when downloading the protein structure under study, COMT (PBD: 4XUC) [27] from the Protein Data Bank (https://www.rcsb.org.) Using PxRy and Discovery Studio software, the ligands and standard medicines were compared to the crystal structure of Catechol-O-Methyltransferase (COMT) (PBD: 4XUC) [27] to determine their molecular docking and binding affinity scores. The presence of water molecules, ligands, and other co-factors was eliminated using the Discovery Studio software. Equation 3 displays the inhibition constant  $(K_i)$  µM of the standard medicines and ligands. The calculation of their binding affinities  $(\Delta G)$  kcal/mol is based on this information, where T=298.15 K is the absolute temperature, R is the gas constant,  $K_i$  is the inhibition constant, and  $\Delta G$  is the binding energy. Good binding affinity ligands were used in subsequent studies such as ADMET, Geometries Molecular Description of the Studied Ligands (DFT), and Prediction of Activity Spectra of Substances Database (PASS) for Biological Activity (PASS).

## 3. Results and discussion

# 3.1. Stereochemical validation of Catechol-O-Methyltransferase's (PDB ID:4XUC) binding pocket crystal structure of (COMT)

The protein Catechol-O-Methyltransferase (COMT) plays a critical modulatory role in the pathophysiology of septic shock, regulating catecholamine metabolism. By inactivating catecholamines such as dopamine and norepinephrine, key mediators of the cardiovascular response in septic shock, COMT influences both hemodynamic stability and immune function [31]. Altered COMT activity correlates with dysregulated catecholamine levels, contributing

to cardiovascular dysfunction and immune imbalance in septic patients [32]. Targeting COMT may offer a novel therapeutic strategy to modulate endogenous catecholamines and support cardiovascular function, providing an alternative or complement to direct adrenergic receptor agonists [33].

We validated this protein using tools such as the Ramachandran plot and MolProbity (Fig. 3 and **Table 1**). The resulting Ramachandran plot suggested a reasonably valid structural model, given the predominance of residues in favored/allowed zones [34] and the  $\phi$ – $\psi$  torsion angles for all residues in the structure. The plot revealed which combinations of  $\phi$  and  $\psi$  angles are sterically allowed, referencing empirically favored (core) and less-favored but permissible regions, as well as banned zones where steric clashes and unfavorable energetics occur. Ramachandran plot hues represent the different regions described in [35]. For COMT, most residues adopt energetically favorable conformations within the plot's red (most favored), orange (allowed), or yellow (generously allowed) areas, suggesting that, structurally, the protein is properly folded and well-refined. The red area of the plot marks the protein core regions, representing the most favorable combinations of  $\phi$ – $\psi$  values with the most energetically stable conformations. These are typically associated with  $\alpha$ -helix and  $\beta$ -sheet secondary structures. The percentage of residues in the core regions is an indicator of stereochemical quality. Protein structure was validated using MolProbity to ensure its suitability for the molecular docking analysis (Table 1).

#### 3.2. Molecular docking analysis

The tools PyRx and Biovia Discovery Studio assisted the investigation of potential Septic Shock inhibitors and the ligands. Compound binding affinities and inhibition constants with the protein COMT 4XUC were obtained from their docking against Septic Shock. According to its crystal structure, Catechol-O-Methyltransferase (COMT - PBD: 4XUC) spanned 80.5073 Å, 66.1331 Å, and 25.0000 Å along the x, y, and z grids, respectively. Its grid center sizes were 35.9837 Å, 31.6925 Å, and 59.0081 Å, respectively. An inhibitory value of a possible active medication should fall between 0.1  $\mu$ M and 1.0  $\mu$ M and not exceed 10 nM [36].

The inhibition constant (Keq) was obtained using the formula Keq =  $\exp[\Delta G/nRT]$  (see Equations 1–3), where R is the gas constant, T is the temperature in Kelvin, n is the number of moles, and  $\Delta G$  is the binding energy. For all assessed ligands, inhibition constants varied from 0.04 to 3.00  $\mu$ M, whereas their binding affinity/scoring energy ranged from -5.2 kcal/mol to -8.6 kcal/mol, as shown in **Table 2**.

$$\Delta G = -nRT \ln \text{Keq} \tag{1}$$

$$Keq = e^{-\left[\frac{\Delta G}{nRT}\right]} \tag{2}$$

$$Ki = \frac{1}{Keq}$$
 (3)

Table 1. MolProbity Validation Metrics of Catechol-O-Methyltransferase (COMT) (PDB ID:4XUC)

	Poor rotamers	0	0.00%	Goal: <0.3%			
	Favored rotamers	178	96.22%	Goal: >98%			
	Ramachandran outliers	0	0 0.00% Goal: <0.0				
Protein	Ramachandran favored	208	96.30%	Goal: >98%			
Geometry	Rama distribution Z-score	$-0.24 \pm 0.54$		Goal: $abs(Z score) < 2$			
	$C\beta$ deviations >0.25Å	1	Goal: 0				
	Bad bonds	5 / 1793	0.28%	Goal: 0%			
	Bad angles	ene-33	0.04%	Goal: <0.1%			
<b>Peptide Omegas</b>	Cis Prolines	01-sep	11.11%	Expected: ≤1 per			
				chain, or ≤5%			
Additional	litional Chiral Hardness swaps		0.43%	See chiral volume			
validations				report for details			

**Table 2.** Binding affinity  $(\Delta G)$  and inhibition constant  $(K_i)$  values of ligands.

Ligand Code	Ligand	Binding affinity $\Delta G$ (kcal/mol)	Inhibition constant K (μM)	$K_i$
L1 (SD1)	Dobutamine	-7.0	7.35	
L2 (SD2)	Dopamine	-5.8	55.77	
L3	Piperlonguminine	-8.0	1.35	
L4	Benzylamine	-5.2	53.63	
L5	Capsaicine	-7.9	1.60	
L6	Gingerenone A	-8.1	1.14	
L7	M-Coumaric acid	-6.6	14.45	
L8	Nobiletin	-7.3	3.74	
L9	O-Coumaric acid	-6.5	17.10	
L10	Piperine	-8.6	0.48	
L11	Pterostilbene	-7.7	2.25	
L12	Rubemanine	-8.0	1.35	
L13	Vanillic Acid	-5.9	47.10	
L14	Zingerone	-6.5	17.10	
L15	Gamma-Bisabolene	-7.1	5.01	
L16	Cystdine	-6.6	14.45	
Co-ligand	Co-ligand	-8.8	0.24	

The ligands Piperlonguminine (L3), Capsaicine (L-5), Gingerenone A (L-6), and Piperine (L-10) emerged as promising potential Septic Shock inhibitors. The predicted amino acid residues participating in the bonding interactions of the target protein COMT (PBD: 4XUC) with the assessed ligands Capsacine (L-5), Gingerenone A (L-6), and Piperine (L-10) and the two standard drugs, Dopamine (SD-2) and Dobutamine (SD-1) are shown in **Table 3**.

Ligand	Amino acid residues involved in the interaction	Types of bonding interaction involved
code		
L-5	ALA A-226, PRO A-224, PRO A-227, LYS A-194	Alkyl
L-6	ASP A-195, PRO A-227, PRO A-229, CYS A-225,	Van der Waals interaction
	LYS A-194	
L-10	TYR A-193, GLU A-140, HIS A-192, GLY A-116	Carbon hydrogen bond, Pi-Pi stacked,
		Pi-Anion
SD-2	MET A-90, LEU A-248, GLY A-249, TRP A-88,	Van der Waals interaction, Pi-Anion
	ASN A-220, CYS A-223	
SD-1	TRF A-293, ASP A-195, LYS A-194, PRO A-224,	Conventional hydrogen bond, Van der
	PRO A-227, ALA A-226, CYS A-225	Waals interaction, Pi-Anion, Pi-Sigma,

Table 3. Amino acid residues and bonding interactions of COMT (PBD: 4XUC) with ligands

When assessed against the target protein COMT (PBD: 4XUC), Capsacine obtained a binding affinity of -7.9 kcal/mol with an inhibition constant of 1.60  $\mu$ M, and Gingerenone A obtained a binding affinity of -8.1 kcal/mol with an inhibition constant of 1.14  $\mu$ M. Piperine's binding affinity was -8.6 kcal/mol with an inhibition constant of 0.48  $\mu$ M, while Rubemanine had a binding affinity of -8.0 kcal/mol with an inhibition constant of 1.35  $\mu$ M. In contrast, Dobutamine and Dopamine had binding affinities of -7.0 kcal/mo and -5.8 kcal/mol with inhibition constants of 7.35  $\mu$ M and 55.77  $\mu$ M, respectively. The 2D interactions of the three most promising ligands (L-5, L-6, and L-10), as well as those of the standard drugs (SD-1 and SD-2) with the receptor, are depicted in **Fig. 4**.

Pi–Alkyl, Alkyl

# 3.3. Biological Activity prediction of the assessed bioactive compounds used in septic shock treatment.

The PASS (Prediction of Activity Spectra for Substances) tool forecasted the biological activity spectra of the assessed bioactive compounds. These predictions rely on the SAR analysis of a training set of more than 205 000 compounds exhibiting above 3 750 different biological activities. The probabilities of having a given biological activity, Pa and Pi, vary from 0.000 to 1.000, and, in general, Pa + Pi  $\neq$  1, since these two probabilities are calculated independently [37, 38]. The PASS tool can predict several possible biological activity types for multiple substances, even if these substances do not belong in the same chemical classes. PASS predicts simultaneously pharmacological effects, mechanisms of action, mutagenicity, carcinogenicity, teratogenicity, and embryotoxicity based exclusively on the structural formula of a substance [39].

The canonical SMILES of the assessed compounds with the high binding affinities, Capsaicin (L-5), Gingerenone A (L-6), and Piperine (L-10), and the two reference bioactive compounds, already used to treat septic shock, Dopamine (SD-2) and Dobutamine (SD-1) were obtained from the PubChem database and then submitted to the activity spectrum prediction web tool (www.https://pharmaexpert.ru.passonline/) (PASS). The obtained PASS for biological activity against septic shock of the assessed compounds with the highest budding affinities:, are displayed in **Table 4**.

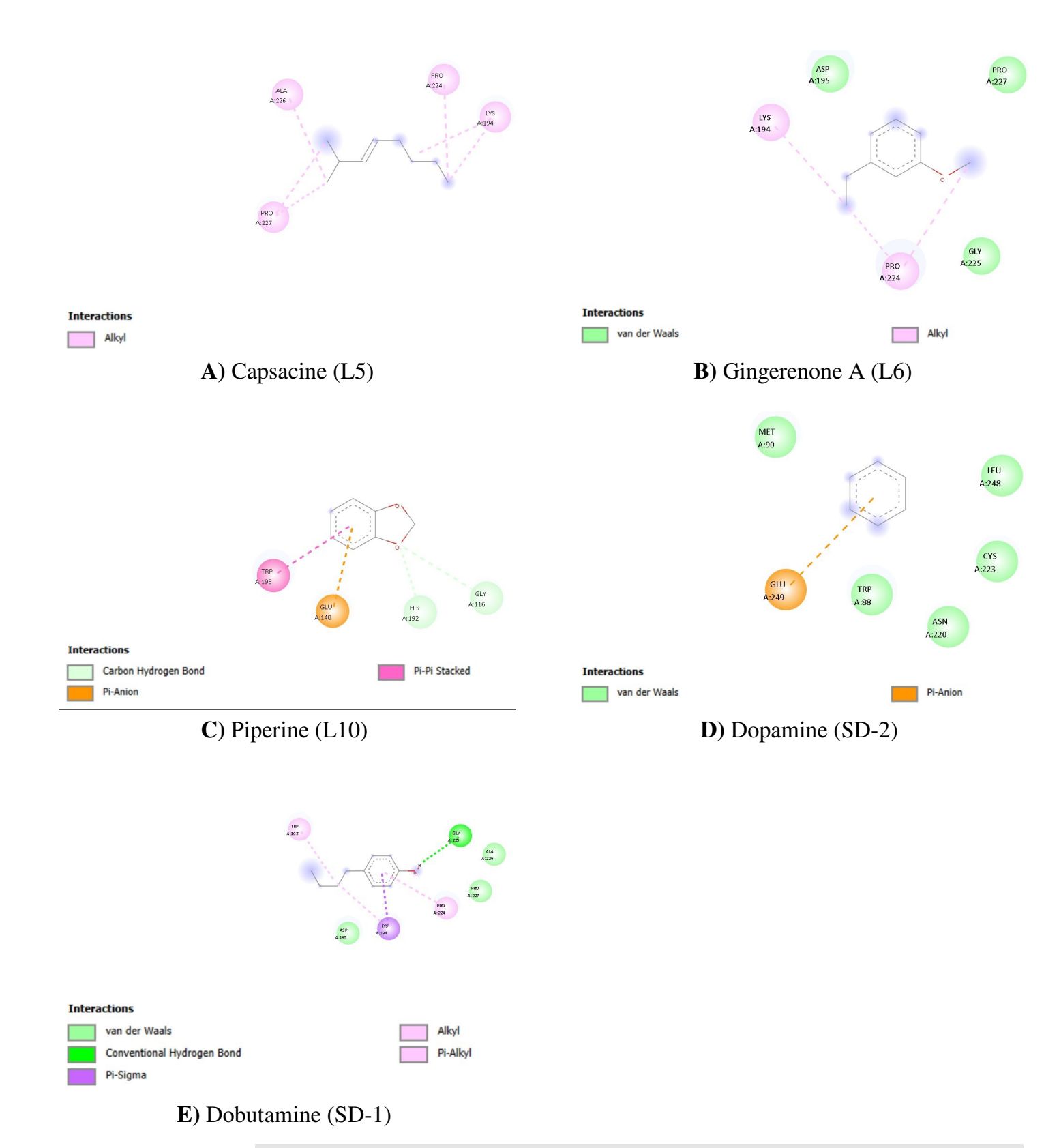


**Figure 4.** 2D interactions of ligands (**A**) L-5, (**B**) L-6, (**C**) L-10, (**D**) SD-2, and (**E**) SD-1 with the receptor protein, COMT (PBD: 4XUC).

Piperine (L-10)

Dopamine (SD-2)

Dobutamine (SD-1)

Ligand	Probability to be active (Pa)	Probability to be inactive (Pi)
Capsacine (L-5)	0.351	0.017
Gingerenone A (L-6)	0.346	0.017

0.069

0.101

0.265

Table 4. Prediction of activity toward septic shock for selected ligands and two standard drugs.

0.200

0.169

0.279

With a probability of being active for treating septic shock (Pa = 0.351), Capsacine (L-5) ranked as the most promising assessed ligand, and Gingerenone A (L-6) followed with a Pa of 0.346. (Table 4). Compared to the two assessed conventional medications (Dopamine and Dobutamine), these two compounds Capsacine (L-5) and Gingerenone A (L-6) obtained higher probabilities of being active in treating septic shock.

The probabilities of being active (Pa) and being inactive (Pi) are often used in computational chemistry, drug discovery, and bioinformatics to predict the likely biological functions of a given compound. The probability of being active (Pa) reflects the likelihood of a particular compound, ligand or molecule to exhibit a special biological activity while the probability of being inactive (Pi) predicts how unlikely that compound is to fulfill a specific biological activity. According to [40], if Pa is less than 0.7, the substance is very likely to exhibit a given biological activity, if 0.5 < Pa < 0.7, the substance is likely to exert that activity, and if Pa < 0.5, the substance is very unlikely to exhibit the activity. Comparing Pa to Pi, if Pa > Pi, the compound is more likely to show the predicted activity. PASS is trained primarily on chemical structures and their known activities from public databases, which may underrepresent certain clinically used drugs, especially small endogenous molecules like Dopamine. The ligands studied may share structural motifs with compounds more frequently represented in the PASS training set, leading to higher predicted activities. PASS does not account for pharmacokinetic, metabolic, or receptor subtype-specific effects, which are critical for clinical efficacy. As shown in Table 4, Capsacine (L-5) and Gingerenone A (L-6) are more likely to be active than inactive toward septic shock, given their obtained Pa > Pi values. Piperine (L-10) had a low Pa value, suggesting a weak activity for septic shock; however, its Pa was still greater than its Pi. Regarding the two FDA-approved standard drugs, Dopamine (SD-2) and Dobutamine (SD-1), both showed relatively low probabilities of being active for septic shock, implying that the two commercial drugs do not exhibit biological activity for septic shock.

#### 3.4. Ligand Physiochemical and ADMET properties

The ADMET parameter (*i.e.* drug-likeness and pharmacokinetic properties) results for the ligands Capsaicin, Gingerenone, Piperine, and the standard drugs, Dopamine, Dobutamine, as revealed by the SwissADMET tool are shown in **Table 5** and **Table 6**.

The Lipinski filter, also known as Lipinski's rule of five (Ro5), evaluates small molecules based on five attributes with established cut-off values using their physicochemical property profiles. To pass the Lipinski filter, molecules must satisfy these conditions: rotatable bonds (ROTBs  $\leq$  10), molecular weight (150  $\leq$  MW  $\leq$  500), lipophilicity (log  $P \leq$  5), hydrogen bond donors (HBD  $\leq$  5), and hydrogen bond acceptors (HBA  $\leq$  10) [41,42]. Capsacine (L-5),

**Table 5.** Drug-likeness and toxicity analysis of selected ligands and two standard drugs.

Ligand	L-5 (Capsacine)	L-6 (Gingerenone A)	L-10 (Piperine)	SD-2 (Dopamine)	SD-1 (Dobutamine)
Formula	$C_{18}H_{27}NO_3$	$C_{21}H_{24}O_5$	$\mathrm{C}_{17}\mathrm{H}_{19}\mathrm{NO}_3$	$C_8H_{11}NO_2$	$C_{18}H_{23}NO_3$
Mass	305.41	356.41	285.34	301.38	153.18
TPSA	58.56	75.99	38.77	72.72	66.48
Rotatable bonds	10	9	4	7	2
XLogP3	3.58	3.74	3.46	3.43	-0.98
WLogP	3.64	3.81	2.51	2.96	0.60
ESOL LogS	-3.53	-4.15	-3.74	-3.81	-0.44
ESOL Class	Soluble	Moderately soluble	Soluble	Soluble	Very soluble
Lipinski violations	0	0	0	0	0
Bioavailability score	0.55	0.55	0.55	0.55	0.55
PAINS alert	0	0	0	1	1
Fraction Csp <sup>3</sup>	0.50	0.29	0.35	0.33	0.25
Synthetic accessibility	2.32	2.74	2.92	2.43	1.01

Table 6. Drug-likeness of the assessed ligands and two standard drugs.									
COMP	НА	MW	RO5	HBD	HBA	MI LOG P			
L-5	22	305.41	0	2	3	3.15			
L-6	26	356.41	0	2	5	3.60			
L-10	21	285.34	0	3	4	3.38			
SD-1 (Dobutamine)	22	301.38	0	4	4	2.36			
SD-2 (Dopamine)	11	153.18	0	3	3	1.27			

L-5 (Capsaicin), L-6 (Gingerenone A), L-10 (Piperine), SD-2 (Dopamine), and SD-1 (Dobutamine).

Gingerenone A (L-6), Piperine (L-10), and the two conventional pharmaceuticals, Dopamine (SD-2) and Dobutamine (SD-1), satisfied the conditions for hydrogen bond donor, hydrogen bond acceptor, and molecular weight. Additionally, these compounds had a bioactivity score of 0.55,  $ROTBs \le 10$ ,  $TPSA \le 131.6$  Å, and  $WLogP \le 5.88$ .

The obtained synthetic accessibility (SA) scores revealed that all ligands can be synthesized, with values ranging between 1.01 and 2.92 (Table 5). SA values range from 1 to 10, whereby a score of 1 stands for easy to synthesize, and 10 means not readily synthesizable. The lowest SA value of 1.01 was obtained by Dobutamine (SD-1), implying it is the easiest to synthesize. Piperine (L-10), at the other end, had an SA value of 2.92, suggesting it is challenging to synthesize.

However, this SA value is still within the synthetically feasible range. Regarding compound solubility, Dobutamine (SD-1) revealed the highest solubility, with a LogS of -0.44. Capsacine (L-5) obtained the second-best solubility score (LogS = -3.53), and together with Piperine (L-10) and Dopamine (SD-2), was deemed soluble. Lastly, Gingerenone A (L-6) ranked last, as moderately soluble (LogS = -4.15).

Dobutamine (SD-1) had a low lipophilicity (XLogP3 = -0.98), which may affect its membrane permeability. Capsacine (L-5), Gingerenone A (L-6), Piperine (L-10), and Dopamine (SD-2) exhibited moderate lipophilicities, with XLogP3 values ranging between 3.4 and 3.7. Capsaicin (L-5), Gingerenone A (L-6), and Piperine (L-10) scored 0 for PAINS alert, while the two commercial drugs scored 1 (Table 5).

Even though all three ligands passed the Lipinski filter, indicating good oral bioavailability potential, Capsacine (L-5) ranked best among ligands, with no PAINS alert, good solubility, moderate lipophilicity, and good synthetic score and LogP values (Table 5 and Table 6), becoming the top candidate for oral drug potential. Gingerenone A (L-6) scored low for solubility but remained drug-like, and Piperine (L-10) was a good candidate, although slightly challenging to synthesize.

## 3.5. Ligand geometries based on their calculated molecular descriptions

Density Functional Theory (DFT) at ground state in the aqueous phase was utilized to optimize the assessed compounds and determine their reactivity descriptor. The molecular descriptions, which include the dipole moment (DM), the electron affinity (EA), the ionization potential (IP), the chemical potential  $(\mu)$ , the chemical hardness  $(\eta)$ , chemical softness (S), electronegativity  $(\chi)$ , electrophilicity  $(\omega)$ , the electron donating power  $(\omega^-)$ , the electron accepting power  $(\omega^+)$ , and the global electrophilicity index  $(\Delta\omega^\pm)$ , were calculated and are displayed in **Table 7** and **Table 8**.

A compound's chemical reactivity derives from the assessment of its lowest unoccupied molecular orbital (LUMO) and its highest occupied molecular orbital (HOMO) (see Equations 4 to 14). LUMO indicates that a compound is absorbing electrons, whereas HOMO signals that a molecule is donating electrons. For the tested ligands, a high HOMO value indicated that they may attach to the receptor with ease. The global electrophilicity index, chemical potential, and dipole moment (DM) contributed to the ligand's increased stability in the protein-ligand complex. The HOMO and LUMO energies primarily describe the global chemical reactivity of a molecule, offering a qualitative insight into how electronically adaptable a ligand might be when interacting with the binding site of a receptor. A higher HOMO energy may suggest better potential for interacting with electron-deficient residues, and a lower LUMO may indicate greater electrophilic adaptability. The differences between HOMO and LUMO underlie Band gap (BG) and dipole moment calculations. Fig. 5 shows the chemical structures of Capsacine (L-5), Gingerenone A (L-6), and Piperine (L-10), while Fig. 6 shows the HOMO, LUMO, and Molecular Electrostatic Potential (MEP) for these ligands.

<b>Table 7.</b> Ligand o	ptimization in	water phase.
--------------------------	----------------	--------------

Ligand	H (eV)	L (eV)	BG	LOG P	DM	PSA	MW	$\mathbf{A}(\mathbf{A}^2)$	$\mathbf{V}(\mathbf{A}^3)$	P
L-5 (Capsacine)	-5.96	-0.11	5.85	1.32	2.19	51.728	305.41	387.77	347.40	68.17
L-6 (Gingerenone A)	-5.63	-1.43	4.20	-0.01	5.33	63.873	356.41	412.58	379.53	71.17
L-10 (Piperine)	-5.43	-1.90	3.53	0.46	5.07	31.616	285.54	322.78	302.24	65.06

**Note:** H (HOMO), L (LUMO), BG (Band gap), DM (Dipole moment), PSA (Polar Surface Area), MW (Molecular Weight), A (Area), V (Volume), P (Polarizability).

Table 8.	Ligand	molecular	description:	s in water phase.
----------	--------	-----------	--------------	-------------------

Ligand	S	EA	IP	μ	η	ω	χ	$\omega^{-}$	$\omega^+$	$\Delta\omega^{\pm}$
L-5 (Capsacine)	0.17	0.11	5.96	3.03	2.92	1.57	-3.03	-3.45	-0.42	-3.87
L-6 (Gingerenone A)	0.23	1.43	5.63	3.53	2.10	2.96	-3.53	-4.99	-1.46	-6.45
L-10 (Piperine)	0.28	1.90	5.43	3.66	1.76	3.80	-3.66	-5.85	-2.91	-7.76

**Note:** S (Softness),  $\omega$  (Electrophilicity), IP (Ionization Potential),  $\mu$  (Chemical Potential),  $\eta$  (Chemical Hardness),  $\chi$  (Electronegativity),  $\omega^-$  (Electrophilic Attack Index),  $\omega^+$  (Nucleophilic Attack Index). See section 3.5 for descriptor definitions.

**A)** Chemical structure of Capsacine (L-5)

**B**) Chemical structure of Gingerenone A (L-6)

C) Chemical structure of Piperine (L-10)

Figure 5. Chemical structures of Capsacine (L-5), Gingerenone A (L-6) and Piperine (L-10).

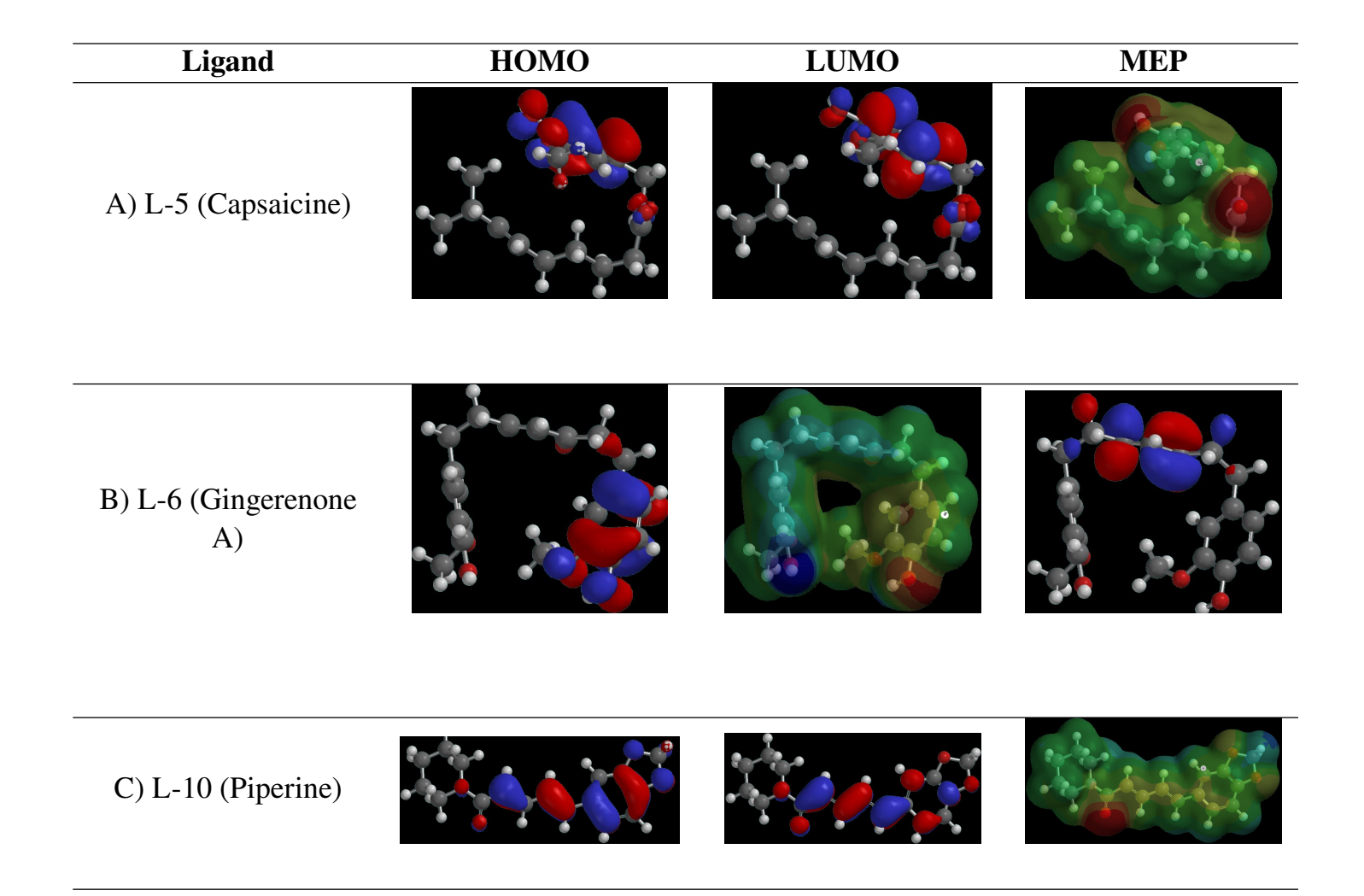


Figure 6. Representations of the assessed Ligands' HOMO, LUMO and Molecular Electrostatic Potential (MEP).

Using Molecular Electrostatic Potential (MEP) mapping, ligand regions of positive and negative charges were visualized, facilitating the identification of areas likely to participate in hydrogen bonding, electrostatic, or  $\pi$ -interactions with the receptor. Overlaying MEP maps with protein binding pockets aids in rationalizing docking poses. Table 8 provides details on chemical softness, electrophilicity, ionization potential, chemical potential, chemical hardness, electronegativity, electrophilic attack index, and nucleophilic attack index of the assessed ligands, Capsacine (L-5), Gingerenone A (L-6), and Piperine (L-10). Since chemical softness (S) explains reactivity, the higher the value of chemical softness, the higher the reactivity. Among the three ligands, Piperine (L-10) had the highest chemical softness, followed by Gingerenone A (L-6) and Capsacine (L-5), implying that Piperine (L-10) is the most reactive of the three ligands.

Electron potential (EP) is the energy change occurring when an atom gains an electron in its gaseous state, and the ionization potential (IP) is the amount of energy required to remove an electron from a neutral atom in its gaseous state. Chemical Potential is the tendency of an electron to escape; the more negative the value of chemical potential, the more stable the compound. Chemical hardness is a compound's resistance to changing its electron distribution; the higher the chemical hardness value, the more stable the compound. Electronegativity is the tendency of a compound to attract electrons. The electrophilic attack index is the tendency of a compound to

undergo electrophilic attack, while the nucleophilic attack index is the tendency of that compound to undergo a nucleophilic attack. Capsaicin (L-5) showed a low reactivity, moderate stability, and a weak nucleophilic/electrophilic behavior. Gingerenone A (L-6) demonstrated stronger electrophilicity, higher reactivity, and potential as an electron acceptor. Piperine (L-10) had the highest reactivity and electrophilicity, emerging as a strong candidate for bio-interaction.

Active compounds exhibit narrow HOMO–LUMO gaps. Among the assessed compounds, Piperine (L-10) had the narrowest HOMO–LUMO gap value, followed by Gingerenone A (L-6) and Capsaicin (L-5) respectively (Table 7). A narrow HOMO–LUMO gap indicates higher chemical reactivity, which may facilitate stronger interactions in the binding site during docking.

$$E_g = E_{\text{HOMO}} - E_{\text{LUMO}}(eV) \tag{4}$$

$$EA = -E_{\text{LUMO}}(eV) \tag{5}$$

$$IP = -E_{\text{HOMO}}(eV) \tag{6}$$

$$\eta = \frac{IP - EA}{2} \tag{7}$$

$$S = \frac{1}{2n} (eV) \tag{8}$$

$$\mu = \frac{IP + EA}{2} \tag{9}$$

$$\omega = \frac{\mu^2}{2n} \tag{10}$$

$$\chi = -\mu \tag{11}$$

$$\omega^{+} = \frac{(IP + 3EA)^{2}}{16(IP - EA)} \tag{12}$$

$$\omega^{-} = \frac{(3IP + EA)^2}{16(IP - EA)} \tag{13}$$

$$\Delta \omega^{\pm} = \omega^{+} - (-\omega^{-}) \tag{14}$$

# 4. Conclusion

Sepsis can progress to septic shock when treatment is delayed, and rapidly increase mortality rate by 50 %. Prompt diagnosis and treatment are essential to increase the survival rate of septic patients. Low-income countries, have a high burden of infectious diseases, malnutrition, and limited healthcare resources [43, 44]. The traditional clinical methods of producing a drug are time and resource consuming, and the drug may fail all the clinical trial, leading to fruitless efforts. The *in-sillico* analysis in this study showed that the bioactive compounds Capsacine (L-5), Gingerenone A (L-6) and Piperine (L-10), possess better binding affinities to the target protein Catechol-O-Methlytransferase (PBD: 4XUC) than the approved drugs Dobutamine and Dopamine. Therefore, these bioactive compounds can serve as a potential therapeutic drug for the treatment of septic shock.

Asibor, et al., 2025

# 5. Acknowledgments

The Authors acknowledge the Department of Pure and Applied Chemistry, at Ladoke Akintola University of Technology for having made available its computational facilities.

# 6. Availability of Data and Material Statement

All data generated or analyzed during this study are included in this article.

### 7. Conflicts of Interest

There is no conflict of interest regarding the publication of this article.

#### References

- [1] Akinade A. Assessment of the Effect of Ethylacetate Extract of *Plumbago zeylanica* on Mitochondria Permeability Transition Pore, *European Journal of Biology*, 8(1):54–70, 2023. https://doi.org/10.47672/ejb.1699
- [2] Nwanze P. I., Nwaru L. M., Oranusi S., Dimkpa U., Okwu M. U., Babatunde B. B., Anake A., Jatto W., Asagwara C. E. Urinary Tract Infection in Okada Village: Prevalence and Antimicrobial Susceptibility Pattern, *Scientific Research and Essays*, 2(4):112–116, 2007.
- [3] Shopsin B., Kreiswirth B. Molecular epidemiology of methicillin resistant *Staphylococcus aureus*, *Emerging Infectious Diseases*, 7(2):323–326, 2001.
  - https://doi.org/10.3201/eid0702.010236
- [4] Funk D. J., Parrillo J. E., Kumar A. Sepsis and Septic Shock: A History, *Critical Care Clinics*, 25:83–101, 2009.
  - https://doi.org/10.1016/j.ccc.2008.12.003
- [5] Rodríguez A., Martín Loeches I., Yébenes J. C. New definition of sepsis and septic shock: What does it give us? *Medicina Intensiva*, 41:38–40, 2017.
  - https://doi.org/10.1016/j.medin.2016.03.008
- [6] Gorecki G., Cochior D., Moldovan C., Rusu E. Molecular mechanisms in septic shock, *Experimental and Therapeutic Medicine*, 22:1161, 2021.
  - https://doi.org/10.3892/etm.2021.10595
- [7] Simon T. P., Thiele C., Schuerholz T., Fries M., Stadermann F., Haase G., Amann K. U., Marx G. Molecular weight and molar substitution are more important in HES-induced renal impairment than concentration after hemorrhagic and septic shock, *Minerva Anestesiologica Journal*, 81(6):608–618, 2015.
- [8] Peng Y., Zhang W., Xu Y., Li L., Yu W., Zeng J., Ming S., Fang Z., Wang Z., Gao X. Performance of SOFA, qSOFA and SIRS to predict septic shock after percutaneous nephrolithotomy, *World Journal of Urology*, 39(2):501–510, 2021.

- https://doi.org/10.1007/s00345-020-03183-2
- [9] Lee W. L. Reply to Mehmood: Adrenomedullin: A Double-edged Sword in Septic Shock and Heart Failure Therapeutics? *American Journal of Respiratory and Critical Care Medicine*, 201(9):1165, 2020.
  - https://doi.org/10.1164/rccm.202001-0072LE
- [10] Izumida T., Imamura T. The Impact of Management Using Fluid Response Evaluation on Renal and Respiratory Failure in Septic Shock, *Chest*, 158(6):2706–2707, 2020.
  - https://doi.org/10.1016/j.chest.2020.06.088
- [11] Garrido P., Rovira C., Cueto P., Fort-Gallifa I., Hernández-Aguilera A., Cabré N., Luciano-Mateo F., García-Heredia A., Camps J., Joven J., Garcia E., Vallverdú I. Effect of continuous renal-replacement therapy on paraoxonase-1-related variables in patients with acute renal failure caused by septic shock, *Clinical Biochemistry*, 61:1–6, 2018.
  - https://doi.org/10.1016/j.clinbiochem.2018.08.010
- [12] Bakker J., Kattan E., Annane D., Castro R., Cecconi M., De Backer D., Dubin A., Evans I., Gong M. N., Hamzaoui O., Ince C., Levy B., Monnet X., Ospina Tascon G. A., Ostermann M., Pinsky M. R., Russell J. A., Saugel B., Scheeren T. W. I., Hernandez G. Current practice and evolving concepts in septic shock resuscitation, *Intensive Care Medicine*, 48(2):148–163, 2022.
  - https://doi.org/10.1007/s00134-021-06595-9
- [13] Singh M., Hussain M. S., Tewari D., Kumar B., Mansoor S., Ganesh N. Antimicrobial Potential of Ethanolic Extracts of Avacado, Allspice, Tejpatta, and Dalchini Against Different Bacterial Strains, *World Journal of Pharmaceutical and Life Science*, 6(9):192–200, 2020.
- [14] Hussain M. S., Singh M., Kumar B., Tewari D., Mansoor S., Ganesh N. Antimicrobial Activity in Ethanolic Extracts of *Bixa orellana L.*, *Simarouba glauca DC.*, and *Ocimum tenuiflorum L.* Collected from JNCH Herbal Garden, *World Journal of Pharmaceutical Research*, 9(4):650–663, 2020.
- [15] Luo S., Gou L., Liu S., Cao X. Efficacy and safety of Shenfu injection in the treatment of sepsis: a protocol for systematic review and meta-analysis, *Medicine*, 100(37):e27196, 2021.
  - https://doi.org/10.1097/md.000000000027196.e27196
- [16] Huang P., Guo Y., Feng S., Zhao G., Li B., Liu Q. Efficacy and safety of Shenfu injection for septic shock: A systematic review and meta-analysis of randomized controlled trials, *The American Journal of Emergency Medicine*, 37(12):2197–2204, 2019.
  - https://doi.org/10.1016/j.ajem.2019.03.032
- [17] Kim E. Y., Park C., Lee G., Jeong S., Song J., Lee D. H. Epidemiological characteristics of varicella outbreaks in the Republic of Korea, 2016–2020, *Osong Public Health and Research Perspectives*, 13(2):133–141, 2022.
  - https://doi.org/10.24171/j.phrp.2022.0087

[18] Yébenes J. C., Ruiz-Rodríguez J. C., Ferrer R., Cleries M., Bosch A., Lorencio C., Rodríguez A., Nuvials X., Martin-Loeches I., Artigas A., SOCMIC. Epidemiology of sepsis in Catalonia: analysis of incidence and outcomes in a European setting, *Annals of Intensive Care*, 19(7):2017.

https://doi.org/10.1186/s13613-017-0241-1

[19] Kumar S., Bhardwaj V. K., Singh R., Das P., Purohit R. Identification of acridinedione scaffolds as potential inhibitor of DENV-2 C protein: An in silico strategy to combat dengue, *Journal of Cellular Biochemistry*, 123(5):935–946, 2022.

https://doi.org/10.1002/jcb.30237

[20] Singh V. K., Bhardwaj P., Das P., Purohit R. Identification of  $11\beta$ -HSD1 inhibitors through enhanced sampling methods, *Chemical Communications*, 58(32):5005–5008, 2022.

https://doi.org/10.1039/D1CC06894F

[21] Bhardwaj V. K., Oakley A., Purohit R. Mechanistic behavior and subtle key events during DNA clamp opening and closing in T4 bacteriophage, *International Journal of Biological Macromolecules*, 208:11–19, 2022.

https://doi.org/10.1016/j.ijbiomac.2022.03.021

[22] Vijayakumar V. R., Rajendran P. J., Poornimaa M., Ramanathan K., Saha T., Das S., Dharumadurai D. Structural geometry, electronic properties and pre-clinical evaluation of antibacterial compounds from lichen-associated *Streptomyces mobaraensis* DRM1 and *Nocardiopsis synnemataformans* DRM2, *Journal of Molecular Structure*, 1312:138561, 2024.

https://doi.org/10.1016/j.molstruc.2024.138561

[23] Yuan H., Liu Y., Huang K., Hao H., Xue Y. T. Therapeutic mechanism and key active ingredients of *Shenfu injection* in sepsis: a network pharmacology and molecular docking approach, *Evidence-Based Complementary and Alternative Medicine*, 2022(1):9686149, 2022.

https://doi.org/10.1155/2022/9686149

[24] Becke A. D. Density-functional thermochemistry. III. The role of exact exchange, *The Journal of Chemical Physics*, 98:5648–565, 1993.

https://doi.org/10.1063/1.464913

[25] Lee C., Yang W., Parr R. G. Development of the Colle–Salvetti correlation-energy formula into a functional of the electron density, *Physical Review B*, 37:785–789, 1988.

https://doi.org/10.1103/PhysRevB.37.785

[26] Jacquemin D., Perpete E. A., Ciofini I., Adamo C. Accurate simulation of optical properties in dyes, *Accounts of Chemical Research*, 42:326–334, 2008.

https://doi.org/10.1021/ar800163d

[27] Allison T., Wolkenberg S., Sanders J. M., Soisson S. M. Synthesis and evaluation of heterocyclic catechol mimics as inhibitors of catechol-O-methyltransferase (COMT): Structure with Cmpd18 (*1-(biphenyl-3-yl)-3-hydroxypyridin-4(1H)-one*), 2015.

https://doi.org/10.1021/ml500502d

[28] Tian W., Chen C., Lei X., Zhao J., Liang J. CASTp 3.0: Computed atlas of surface topography of proteins, *Nucleic Acids Research*, 46(W1):W363–W367, 2018.

https://doi.org/10.1093/nar/gky473

[29] Andreis D. T., Singer M. Catecholamines for inflammatory shock: a Jekyll-and-Hyde conundrum, *Intensive Care Medicine*, 42(9):1387–1397, 2016.

https://doi.org/10.1007/s00134-016-4249-z

[30] Zhu B. Catechol-O-Methyltransferase (COMT)-mediated methylation metabolism of endogenous bioactive catechols and modulation by endobiotics and xenobiotics: importance in pathophysiology and pathogenesis, *Current Drug Metabolism*, 3(3):321–349, 2002.

https://doi.org/10.2174/1389200023337586

[31] Smith B. L., Dunham J. E., Sweeney B. M., Dearing C., Shepherd R. H., Bardgett M. E. Biopsychology Lab: COMT Genotype Associations with Vagal Tone and Frontal Alpha Asymmetry, *Journal of Undergraduate Neuroscience Education*, 23(2):A95, 2025.

https://doi.org/10.59390/SMML6995

[32] Haase-Fielitz A., Haase M., Bellomo R., Lambert G., Matalanis G., Story D., Dragun D. Decreased catecholamine degradation associates with shock and kidney injury after cardiac surgery, *Journal of the American Society of Nephrology*, 20(6):1393–1403, 2009.

https://doi.org/10.1681/ASN.2008080915

[33] Belfiore J., Taddei R., Biancofiore G. Catecholamines in sepsis: pharmacological insights and clinical applications—a narrative review, *Journal of Anesthesia, Analgesia and Critical Care*, 5(1):17, 2025.

https://doi.org/10.1186/s44158-025-00241-2

- [34] Gopalakrishnan K., Saravanan S., Sarani R., Sekar K. RPMS: Ramachandran plot for multiple structures, *Applied Crystallography*, 41(1):219–221, 2008.
- [35] Morris A. L., MacArthur M. W., Hutchinson E. G., Thornton J. M. Stereochemical quality of protein structure coordinates, *Proteins*, 12:345–364, 1992.
- [36] Oyebamiji A. K. et al. Predicting the biological activity of selected phytochemicals in *Alsophila spinulosa* leaves against 4-aminobutyrate-aminotransferase: A potential antiepilepsy agents, *Ecletica Quimica*, 49:1492, 2024.
- [37] Marwaha A., Goel R., Mahajan M. PASS-predicted design, synthesis and biological evaluation of cyclic nitrones as nootropics, *Bioorganic & Medicinal Chemistry Letters*, 17:5251–5255, 2007.

https://doi.org/10.1016/j.bmcl.2007.06.071

[38] Filimonov D. A., Poroikov V. Probabilistic Approaches in Activity Prediction, 2008. https://doi.org/10.1039/9781847558879-00182

- [39] Poroikov V., Filimonov D. A., Borodina Y., Lagunin A., Kos A. Robustness of biological activity spectra predicted by computer program PASS for noncongeneric sets of chemical compounds, *Journal of Chemical Information and Computer Sciences*, 40:1349–1355, 2000. https://doi.org/10.1021/ci000383k
- [40] Lagunin A., Stepanchikova A., Filimonov D., Poroikov V. PASS: Prediction of activity spectra for biologically active substances, *Bioinformatics*, 16(8):747–748, 2000.
- [41] Lipinski C. A., Lombardo F., Dominy B. W., Feeney P. J. Experimental and computational approaches to estimate solubility and permeability in drug discovery and development settings, *Advanced Drug Delivery Reviews*, 23(1–3):3–25, 2001.
  - https://doi.org/10.1016/S0169-409X(96)00423-1
- [42] Lipinski C. A. Lead-and drug-like compounds: the rule-of-five revolution, *Drug Discovery Today: Technologies*, 1(4):337–341, 2004.
  - https://doi.org/10.5772/52642
- [43] Veszelka S., Tóth A., Walter F. R., Tóth A. E., Gróf I., Mészáros M., Bocsik A., Hellinger É., Vastag M., Rákhely G. Comparison of a rat primary cell-based blood-brain barrier model with epithelial and brain endothelial cell lines: Gene expression and drug transport, *Frontiers in Molecular Neuroscience*, 11:166, 2018.
  - https://doi.org/10.3389/fnmol.2018.00166
- [44] Frenk J., Gomez-Dantés O. The triple burden disease in developing nations, *Harvard International Review*, 10, 2011.

# Exploración Computacional De Compuestos Bioactivos Nigerianos Como Posibles Inhibidores Del Choque Séptico.

Resumen: El choque séptico es una condición médica potencialmente fatal caracterizada por una hipotensión severa o niveles elevados de lactato como consecuencia de la sepsis. Este cuadro ocurre a raíz de infecciones bacterianas y virales patogénicas. En este estudio, se evaluaron computacionalmente veintiocho ligandos de origen vegetal para determinar su capacidad de suprimir el choque séptico mediante la interacción con la proteína catecol-O-metiltransferasa (COMT) (PDB: 4XUC), utilizando análisis de acoplamiento molecular (Molecular Docking), PASS, ADMET y DFT. Los resultados del acoplamiento molecular mostraron que los ligandos evaluados, capsaicina (L5) y gingerenone A (L6), presentaron afinidades de unión de -7.9 kcal/mol y -8.1 kcal/mol, con constantes de inhibición de 1.60 μM y 1.14 μM, respectivamente. En comparación, los fármacos estándar dobutamina y dopamina registraron afinidades de unión de -7.0 y -5.8 kcal/mol, con constantes de inhibición de 7.35 μM y 55.77 μM. En el análisis PASS, L5 y L6 mostraron mayores valores de probabilidad de actividad (0.357 y 0.346), y el análisis ADMET clasificó a L5 y L6 como los ligandos más prometedores. Finalmente, la evaluación DFT indicó que L5 y L6 presentaron brechas de energía de 5.58 y 4.20, respectivamente. En conjunto, todos los análisis demostraron que ambos compuestos, L5 y L6, exhibieron una afinidad de unión con el receptor superior a la de los dos fármacos aprobados evaluados, dobutamina y dopamina.

Palabras Clave: acoplamiento molecular; ADMET; compuestos bioactivos; DFT; PASS.

# Exploração Computacional De Compostos Bioativos Nigerianos Como Possíveis Inibidores Do Choque Séptico.

Resumo: O choque séptico é uma condição médica potencialmente fatal caracterizada por hipotensão severa ou níveis elevados de lactato, como consequência da sepse. Esse quadro ocorre como consequência de infecções bacterianas e virais patogênicas. Neste estudo, vinte e oito ligantes de origem vegetal natural foram avaliados computacionalmente para determinar sua capacidade de suprimir o choque séptico por meio da interação com a proteína catecol-O-metiltransferase (COMT) (PDB: 4XUC), utilizando análises de acoplamento molecular (Molecular Docking), PASS, ADMET e DFT. Os resultados do acoplamento molecular mostraram que os ligantes avaliados, capsaicina (L5) e gingerenone A (L6), apresentaram afinidades de ligação de -7,9 kcal/mol e -8,1 kcal/mol, com constantes de inibição de 1,60 μM e 1,14 μM, respectivamente. Em comparação, os fármacos padrão dobutamina e dopamina apresentaram afinidades de ligação de -7,0 e -5,8 kcal/mol, com constantes de inibição de 7,35 µM e 55,77 µM. A análise PASS revelou que L5 e L6 apresentaram maiores valores de probabilidade de atividade (0,357 e 0,346), e a análise ADMET classificou L5 e L6 como os ligantes mais promissores. Por fim, a avaliação DFT indicou que L5 e L6 apresentaram lacunas de energia de 5,58 e 4,20, respectivamente. Em conjunto, todas as análises demonstraram que ambos os compostos, L5 e L6, exibiram afinidade de ligação com o receptor superior à da dos dois fármacos aprovados avaliados, dobutamina e dopamina.

Palavras-chave: acoplamento molecular; ADMET; compostos bioativos; DFT; PASS.

#### Yemisi Elizabeth Asibor

Dr. Yemisi Elizabeth Asibor is a dedicated Nigerian academic and researcher specializing in Physical and Computational Chemistry. Her research interests encompass Density Functional Theory, Molecular Docking, PASS, ADME, and Molecular Dynamic Simulations, with a particular focus on applying computational methods to medicinal chemistry and drug discovery. Dr. Asibor has contributed to numerous scientific publications.

### **Dayo Felix Latona**

Dr. Latona Dayo Felix holds Ph.D degree in Physical Chemistry from Obafemi Awolowo University, Ile-Ife, Nigeria. He is an Associate Professor of Physical and Computational Chemistry at Osun State University, Osogbo, Nigeria. He has over fifty research publications to his credit with expertise in Reaction Kinetics, Molecular Docking and Corrosion Science.

## Banjo Semire

Prof. Semire Banjo is a professor of Physical and Computational Chemistry in the Department of Pure and Applied Chemistry, Ladoke Akintola University of Technology, Ogbomoso, Nigeria. He is a distinguished academic, researcher, and a mentor whose career in Chemistry reflects a blend of intellectual rigor, innovative inquiry, and impactful contributions to both science and society. His research encompasses the use of Density Functional Theory (DFT), Quantitative Structure-Activity Relationship, Molecular Modeling and Dynamic Simulations to provide comprehensive insights in the areas of Drug Design and Development, Pharmaceutical and Medicinal Chemistry, with a particular focus on dye-sensitized solar cells (DSSCs), a field in which he has developed novel experimental and computational approaches to improve efficiency and sustainability.